International Journal of Application or Innovation in Engineering & Management (IJAIEM)
Web Site: www.ijaiem.org Email: editor@ijaiem.org
Volume 10, Issue 7, July 2021 **ISSN 2319 - 4847**

Satellite Image Enhancement Using Principal Component Analysis (PCA) Transformation Technique to Maximize the Signal-to-Noise ratio for Hyper-Spectral Data

Dahiru Mohammed Zakari [1], Bubakari Joda [2] Kabiru Abubakar Yahya [3]
[1]Department of Surveying and Geoinfoematics, Adamawa State Polytechnic, Yola, School of Environmental Science, Jambutu
[2]Department. of Elect/Elect Engineering School of Engineering Federal Polytechnic Kaltungo, Gombe State
[3]Department. of Elect/Elect Engineering School of Engineering Federal Polytechnic Kaltungo, Gombe State

ABSTRACT

Image measurements are made at many narrow contiguous wavelength bands, resulting in a complete spectrum for each pixel. The total bands include the: First 70 bands in the visible and near-infrared, and the second with 172 bands in the shortwave infrared region. As result, at levels 1 processing, only 198 of the bands are calibrated; radiometric values in the remaining bands arrest to 0 for most data products. The larger number of spectral bands provides the potentials for derived detailed information on the nature and properties of different surface materials on the ground, but mean difficulty in image processing and a large data redundancy due to high correlation among the adjacent bands. The principal component analysis (PCA) technique has been applied to reduce the data dimension and feature extraction from hyper-spectral data for assessing the biophysical and biochemical parameters With a covariance (or correlation) matrix calculated from the data, it is commonly believed that the eigenvalues and the corresponding eigenvectors computed from the covariance (or correlation) matrix can enhance vegetation variation information in the first PCs. Developed one transformation method called "maximum noise fraction" (MNF) transform to maximize the signal-to-noise ratio when choosing PCs with increase component numbers. Therefore, several MNFs to maximize the signal-to-noise ratio are selected for analysis for hyper-spectral data, Such as for determining end member spectra for spectral mixture analysis. Therefore, the larger number of spectral bands provides the potentials for derived detailed information on the nature and properties of different surface materials on the ground.

Keywords: ***Hyper-Spectral Data, Enhancement, wavelength bands, Maximum Noise Fraction" (MNF)***

1. INTRODUCTION

Land cover information is vital for many planning and management activities. The use of panchromatic, medium-scale aerial photographs to map land cover has been an accepted practice since the 1940s. This was then followed by small scale aerial photographs and satellite images which have been utilized for large area land cover mapping [7]. Advancements in computer technology and the sensor system for capturing data have enabled fine spatial, spectral and temporal resolution to be achieved. This in turn has been influenced the information extraction technique; even in the quantitative approach. The multispectral data analysis used to be an optical quantitative approach for fine spectral resolution satellite data. The spectral characteristics of the land surface are the fundamental principles for land cover classification using remotely sensed data. The spectral features include the number of spectral bands, spectral coverage, and resolution (or bands width). The number of spectral bands used for image classification can range from a limited number of multispectral bands (e.g., four bands in SPOT data and seven bands for Landsat TM) to a minimum number of multispectral bands (e.g., ASTER 14 bands and MODIS with 36 bands). The earth Observing-1(EO1) satellite was launched on the 21st November 2000 as part of NASA's New millennium program (NMP) technology path-finding activities to enable more effective (and less costly) hardware and strategies for meeting earth science mission need only in the 21st century. The advanced land Imager (ALI) is a prototype for a new generation of Landsat-7 Thematic mapper. The sensor maintains similar characteristics to Landsat-7 with a spatial resolution of 30m; however, the swath width is 37km as opposed to 185km (Heam et al., 2001; Wuder et al., 2008). It includes detectors arrays that operate in ten bands, one panchromatic, six in visible and near-infrared radiation (VNIR), and three in shortwave infrared radiation (SWIR), spanning the range from 0.433 to 2.35μm. Hyper-spectral data (e.g. Airborne Visible/Infrared Image spectrometer d E O-1 Hyperion imaging with 242 bands). Recently, the hyperspectral analysis approach was introduced

for extracting features from hyper-spectral data. The multispectral analysis is limited to hyper-spectral data. Hence, applying such an approach to classify hyper-spectral data has been proven to be futile. Therefore, in remote sensing, there are several common issues though, that need to be addressed regularly to achieve valuable outcomes in research, and there is a need to highlight quality data. Thus, hyperspectral sensors can produce data of sufficient spectral resolution for direct identification of materials, whereas the broader bands TM cannot resolve these diagnostics spectral differences. Hence, while a broadband system can only discriminate general's differences among materials types. A Hyperspectral sensor affords the potential for detailed identification of materials and better estimates of their abundance [7]. (Some application areas of hyperspectral sensing include; surface Mineralogy, water quality, Bathymetry soil types and erosion, Vegetation types, plant stress, leaf water content, crop types and condition, Snow and ice properties [7].

1.2 Hyperspectral Transformation

Hyperion is a hyperspectral instrument on the Earth-Observing 1 (EO-1), is the first advance satellite hyperspectral sensor, it possesses the following features; The hyper-spectral characteristics of land surfaces are the fundamental principles for land cover classification using remotely sensed data. The spectral features include the number of spectral bands, spectral coverage, and spectral resolution (or bandwidth). The number of bands used for image classification can range from a limited number of multispectral bands (e.g., four bands in SPOT data and seven for Landsat TM)To a minimum number of multispectral bands (e.g., ASTER with 14 bands and MODIS with 36 bands) Hyperspectral data (e.g., Airborne Visible/infrared Imagine spectrometer and EO-1 Hyperion Images with 224 bands) Ultra spectral remote sensing systems collect data in many hundreds of bands. A large number of spectral bands provides the potential to derive detailed information on the nature and properties of different surface materials on the ground. In addition, image data in narrow many narrow contiguous spectral bands (< 10-nm bandwidth) through the visible and solar-reflected infrared portion of the spectrum [13]. The project exercise will focus on hyper-spectral measures for spectral analysis, therefore we have to look at some of the characterizing features of the sensor. Hyperion is the first advance satellite hyperspectral sensor operating across the full solar-reflected spectrum with nominal spectral coverage from 0.4 to 2,5um which comprises four linear arrays, one for each spectrometer, provide high sensitivity in the 0.4-0.7,0.7-1.2, 1.2-1.8, and 1.8-2.5um region respectively. and 10nm spectral resolution. It is a push broom (along-track measures multispectral image data along a swath beneath the aircraft) instrument, capturing 256 spectral each with 242 spectral bands over a 7.6km swath and 30m spatial resolution. Image measurements are made at many narrow contiguous wavelength bands, resulting in a complete spectrum for each pixel. The total bands include the: First 70 bands in the visible and near-infrared, and the second with 172 bands in the shortwave infrared region. As result, during levels 1 processing, only 198 of the bands are calibrated; radiometric values in the remaining bands arrest to 0 for most data products.

The larger number of spectral bands provides the potentials for derived detailed information on the nature and properties of different surface materials on the ground, but mean difficulty in image processing and a large data redundancy due to high correlation among the adjacent bands. This requires sophisticated digital image processing software for data analysis, (e.g. ENVI, The Environment for Visualizing Imageries; ERDAS Imagine; IDRISI etc.). The software undergoes a series of routines to follow: Data preparation, preprocessing, Data classification and accuracy assessment. Therefore, an increase of spectral bands may improve classification accuracy, but only when those bands are useful in discriminating the classes. Analytical Imagine and geophysics (AIG) has developed methods for the analysis of hyper-spectral data that allow reproducible results with minimal subjective analysis (shown in figure 3). These approaches are implemented and documented within the "Environment for Visualizing Images" (ENVI) software system originally developed by AIG scientists (now an Eastman Kogak/ Research system Inc. (RSI) commercial-off-the-sheif (COST) product) Therefore increase of spectral bands may improve classification accuracy, but only when those bands are useful in discriminating the classes (Thenkabail, Enclona et al. 2004a). These systems can discriminate among earth surface feature that has diagnostic absorption and reflectance characteristics over narrow wavelength intervals that are lost within the relatively coarse bands widths of the various bands of conventional multispectral scanners. Because of the large number of very narrow bands sample, hyper-spectral data enable the use of remote sensing data collection in many, very narrow, continuous spectral bands throughout the visible, near-infrared, mid-infrared and thermal infrared portions of the spectrum. This allows the remote sensor-derived spectral reflectance data to be quantitatively compared with *in situ* spectral reflectance data obtained on the ground using a handheld spectroradiometer. The principal component analysis (PCA) technique has been applied to reduce the data dimension and feature extraction from hyper-spectral data for assessing the biophysical and biochemical parameters with a covariance (or correlation) matrix calculated from the data, it is commonly believed that the eigenvalues and the corresponding eigenvectors computed from the covariance (or correlation) matrix can enhance vegetation variation information in the first PCs. Because PCA does not always produce images that show steadily decreasing image quality with increase component number, [6]. Developed one transformation

method called "maximum noise fraction" (MNF) transform to maximize the signal-to-noise ratio when choosing PCs with increase component numbers. Therefore, several MNFs to maximize the signal-to-noise ratio are selected for analysis for hyper-spectral data, such as for determining end member spectra for spectral mixture analysis.

1.3 ATMOSPHERIC CORRECTION

It is simply reducing the effects of the atmospheric component (Water vapour, Dust, Gasses, etc) on the electromagnetic radiation reflected or emitted from the earth's surface. This approach, however, applied to both airborne and satellite data, requires processing radiance-calibration data into apparent reflectance Fast line-of-sight. Atmospheric Analysis of spectral hypercubes (FLAASH) is a principle atmospheric correction modelling tool in ENVI for retrieving spectral reflectance from hyperspectral and multispectral radiance images FLAASH corrects wavelengths in the visible through near-infrared and short-wave infrared region, up to 25um. Unlike many other atmospheric correction programs that interpolate radiation transfer properties from the precalculated database of modelling results. FLAASH also include the following features; Correction for the adjacency effects (pixel mixing due to scattering of surface-reflected radiance). An option to compute scene-average visibility (aerosol/haze amount). FLAASH uses the most advanced techniques for handling particularly stressful atmosphere conditions, such as the presents of clouds. Cirrus and opaque cloud classification map. Adjustable spectral polishing for artefact suppression. FLAASH support hyperspectral sensors (such as Hy-MAP, AVIRIS, HYDICE, HYPERION, probe-1, CASI, and AISA) and multispectral sensors (such as Landsat, SPOT, IRS, and ASTER). Water vapour and aerosol retrieval are only possible when the image contains bands of inappropriate wavelength positions. In addition, FLAASH can correct images collection I either vertical (nadir) or slant-viewing geometries. Atmospheric Correction Now (ACORN) (AIG, *ACORN User's Guide, Stand Alone Version*. Boulder, et al., CO: Analytical, 2001.), currently used for correction of both airborne and satellite hyper-spectral data. The internal Average Relative Reflectance (IAR) technique was used to carry out the conversion of the hyper-spectral data. The output of this conversion is the relative reflectance and this can be achieved by dividing each pixel spectrum by the overall average spectrum. AIG-Developed Hyperspectral Analysis; AIG-developed hyperspectral analysis. Methods used for both the airborne sensor and Hyperion data (implemented in the ENVI images analysis software) include spectral polishing [3]. spectral data reduction using MNF transformation [6]. spatial data reduction using the pixels purity Index (PPI). An n-Dimension Visualizer to determine image endmembers [3]. densification of endmembers using their reflectance spectra in the spectral Analysis, and mineral mapping using both the spectral Angle Mapper (SAM), and Mixture-Tuned Matched filtering (MTMF) [12]. At this stage, there are two ways of applying atmospheric correction, which includes, Internal Average Relative reflectance (IAR) and Fast line-of-sight Atmospheric Analysis of the spectral hypercube (FLAASH) each simply reducing the effects of the atmospheric component (Water vapour, Dust, Gasses, etc.) on the electromagnetic radiation reflected or emitted from the earth's surface, in this which IAR was applied.

2. DATA PREPARATION AND PREPROCESSING

However, to use hyper-spectral data properly, it is generally accepted that the data must be radiometrically corrected. In addition to removing the atmospheric effect, this process involves transforming the hyperspectral data from at sensor radiance to scale surface reflectance [9], Image preprocessing may include the examination of image quality, Removal of striping, Conversion of a digital number to reflectance, and geometric rectification. After radiometric correction, there is still a pronounced vertical striping pattern in the Hyperion data, such striping is often seen in data acquired using push broom technology [12].

2.1 STRIPING

Striping in satellite data can be as result arise due to many artefacts such as failure of the sensor, saturation of detectors, cut off for some time or permanent defect in the scan line correctors (ETM+) spots, or vibration in imagery by identifying periodicities (areas of high spatial frequency) [15]. Regular errors in data such as those caused by sensor anomalies (e.g., striping) can be removed using Fourier editing. The artefacts caused by the striping are a hindrance to image processing and classification/ feature extraction. The removal of these stripes in spatial domains difficult because their removal changes values of surrounding pixels as well that are already correct [16]. Fourier transform is not often applied to pattern and object recognition; because of its inefficiency in image description and calculation but stripes are a feature that is easily identifiable through Fourier transforms [4].

2.2 IMAGE DECOMPOSITION/MULTIRESOLUTION ANALYSIS

The basic theory of decomposition is that an image can be converted into high-frequency and low-frequency components.

2.3 IMAGE PROCESSING

Image processing systems consist of specialized hardware and software for the analysis and display of digital images, such systems vary from a very expensive and powerful mainframe system to relatively inexpensive microcomputer systems. These systems often have "user-friendly" menus [13]

2.4 PROCEDURE

Airborne Imaging Spectrometer (AIS), Hyperion and may be caused by factors such as detector nonlinearities, movement of the slit to the focal plane, and temperature effects. Destriping of the Hyperion data was accomplished using custom software (following the model of software written for the original push-broom imaging spectrometer (AIS) [12]. This approach adjusts each image column brightness (in all bands) based on a calculated offset relative to the scene average detector response. Destriping is only required for correcting the push broom Hyperion data.

2.5 METHODS AND PROCEDURES

In this study, two software were used for the available range of techniques in the context of Fourier and wavelet analysis, including ERDAS Imagine 2014, and ENVI 5.0. After analyzing the software most of the project work was done in ENVI 5.0. The frequency-domain de-striping procedure done in ERDAS was by using the Fast Fourier Transform available in the Image Interpreter main menu. The frequency-domain images were edited in the Fourier editor. The available high-pass and low-pass filters were applied depending upon the data and the shape of the frequency to be suppressed or enhanced. Circular, rectangular, wedge-shaped tools were used from the available shapes to cut-off portions. The Edited layers were turned back to images using the Inverse Fast Fourier Transform to obtain the de-striped image and which can be further enhanced.

2.6 MINIMUM NOISE FRACTION (MNF) TRANSFORMATION

The Minimum Noise Fraction (MNF) transform is used to determine the inherent dimensionality of image data, to segregate noise in the data, and to reduce the computational requirements for subsequent processing This analysis approach of minimum noise fraction (MNF) transformation consist of spectral compression, Noise suppression and dimensionality reduction [12]. The transformation applies two cascaded principal components analysis [5]; ***To decorrelate and rescales noise in the data,*** this results in transformed data I which noise has unit variance and no band-to-band correlation.

3. HYPER-SPECTRAL DATA DIMENSIONALITY AND NOISE REDUCTION

From the MNF results, the first four transformed bands (MNF1- MNF4) contained more information and the spatial coherency decrease significantly with the increase of MNF band number (Figure 1).

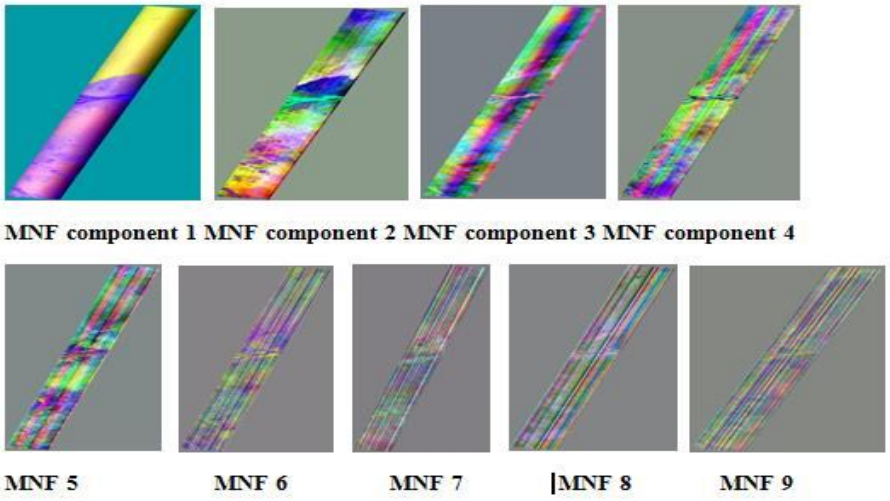

Figure 1. Minimum Noise Fraction

The Eigen-images (MNF bands) extracted information in the Eigen information from Hyperion data, as the MNF Eigen- decreases images increase, the value and the coherent

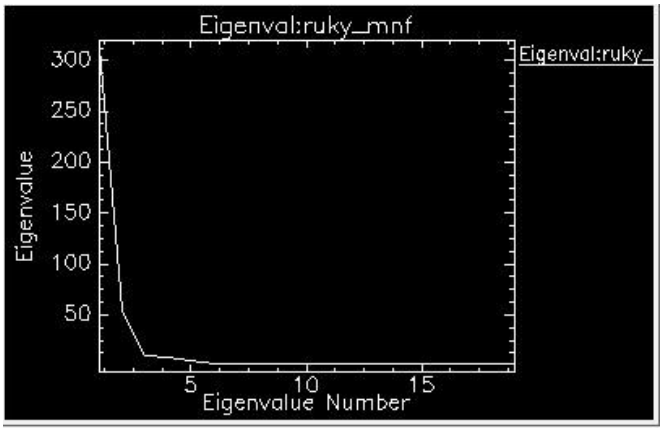

Figure 2. Eigen Values of MNF Transformed Bands and Bands Number

Table 1. Dims: Full Scene (3,652,000 points)

Basic Stats	Min	Max	Mean	Stdev		Num Eigenvalue
Band 1	**-88.131233**	**10.489872**	**-0.000000**	**17.679356**	**1**	**312.559619**
Band 2	**-47.745426**	**88.345131**	**0.000000**	**7.386905**	**2**	**54.566368**
Band3	**-166.474045**	**16.354576**	**-0.000000**	**3.181249**	**3**	**10.120345**
Band 4	**-43.908859**	**54.822575**	**-0.000000**	**2.830211**	**4**	**8.010094**
Band 5	**-34.068008**	**86.182037**	**0.000000**	**2.221828**	**5**	**4.936521**
Band 6	**-27.927170**	**37.361897**	**-0.000000**	**1.525839**	**6**	**2.328185**
Band 7	**-54.489304**	**48.006470**	**-0.000000**	**1.473587**	**7**	**2.171458**
Band 8	**-25.530287**	**30.961151**	**0.000000**	**1.417373**	**8**	**2.008945**
Band 9	**-31.196659**	**38.471935**	**-0.000000**	**1.401501**	**9**	**1.964206**
Band 10	**-24.807873**	**19.573233**	**0.000000**	**1.350807**	**10**	**1.824681**

Band 11 -22.411642 16.791292	**0.000000**	**1.315150**	**11**	**1.729620**
Band 12 -29.540174 19.163858	**-0.000000**	**1.296701**	**12**	**1.681433**
Band 13 -17.995005 13.585849	**0.000000**	**1.293561**	**13**	**1.673301**
Band 14 -17.433729 15.850491	**-0.000000**	**1.278794**	**14**	**1.635314**
Band 15 -16.115385 20.079943	**-0.000000**	**1.263628**	**15**	**1.596755**
Band 16 -11.843556 17.857430	**-0.000000**	**1.259006**	**16**	**1.585095**
Band 17 -24.202747 21.610266	**-0.000000**	**1.255824**	**17**	**1.577094**
Band 18 -14.384565 13.377349	**0.000000**	**1.245620**	**18**	**1.551569**
Band 19 -12.954618 15.344109	**-0.000000**	**1.236825**	**19**	**1.529736**

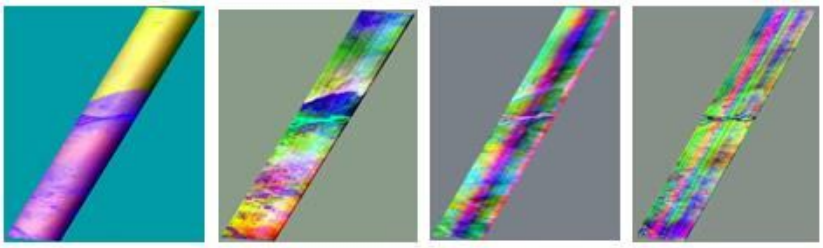

MNF component 1 MNF component 2 MNF component 3 MNF component 4

Figure 3. MNF bands, the information decreased drastically, to almost nearly 95% less than the first MNF band.

3.1 STATISTICAL ANALYSIS

Most researchers have employed statistical analysis methods to correlate biophysical or biochemical parameters with spectral reflectance, or derivative spectra in the visible, NIR, and SWIR wavelengths of hyper-spectral data or plant community level. Therefore, mean, standard deviation variance, minimum values, maximum values, variance-covariance matrix and correlation matrix represent fundamental information on the spectral characteristics of any datasets, *(Table 1, Above and Figure.4a-c*

Delete some of the unwanted redundant band, Transform the data so that the information content is preserved while reducing the dimensionality of the data set.

Mean of $X = \mu = \sum_{i=1}^{N} P_i X_i$, for N values of $X = E(X)$ (1),

where P_i is the probability of the occurrence of

Variance $\Rightarrow \sigma^2 = VAR(X) = \sum_{i=\frac{1}{2}}^{N} P_i (X_i - E(X))^2 or \Rightarrow \sigma^2 = VAR(X) = E\left[(X_i - E(X))^2\right]$ Or

$\Rightarrow \sigma^2 = VAR(X) = (X^2) - (E(X))^2$ (2)

Standard deviation $\Rightarrow \sigma^2 = \sqrt{\sigma^2} = \sqrt{VAR(X) = SD(X)}$ (3)

$COV(X,V) = \sum_{i=1}^{N} P_{xy} (X_i - E(X)(Y_i - E(Y)))$ Or

$\Rightarrow \sigma_{xy} = COV(X,Y) = E\left[(X - E(X))(Y - E(Y))\right]$ (4)

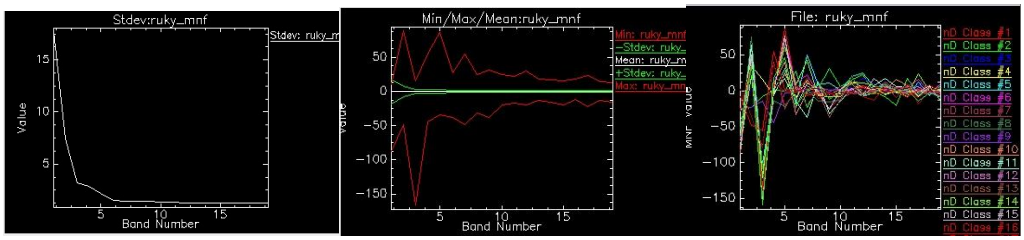

Figure 4a. Standard deviation **Figure 4b.** Min/Max/Mean **Figure 4c**. Eigen Value

Table 2. Eigenvalues computed for the covariance matrix.

Eigenvalues	**1**	**2**	**3**	**4**	**5**	**6**	**7**	**8**	**9**	**10**
312.56	**54.57**	**10.12**	**8.01**	**4.94**	**2.33**	**2.17**	**2.01**	**1.96**	**1.82**	
Difference	**257.99**	**44.45**	**2.11**	**3.07**	**2.61**	**0.16**	**0.16**	**0.05**	**0.14**	

Total Variance can be generated through; $\sum_{p=i}^{n} \lambda_p$

$\sum_{p=1}^{10} \lambda_p \Rightarrow$312.56 + 54.57 + 10.12 + 8.01 + 4.94 + 2.33 + 2.17 + 2.01 +1.96 +1.82= 400.49 (5)

The percentage of variance in the data set can be derived through;

$$\Rightarrow \%_p = \frac{Eigenvalue\ \lambda_p \times 100}{total\ variance\ \sum_{p=i}^{n} \lambda_p} \Rightarrow \% = \frac{312.56 \times 100}{400.49} = 78.44\%\ ,\ \% = \frac{54.57 \times 100}{400.49} = 13.63\% \ldots\ldots n\% \quad (6)$$

TABLE 3

Percentage	**78.44**	**13.63**	**2.53**	**2.00**	**1.23**	**0.58**	**0.54**	**0.50**	**0.50**	**0.45**
Cumulative	**78.44**	**92.07**	**94.60**	**96.60**	**97.83**	**98.41**	**98.95**	**99.45**	**99.95**	**100.00**

3.2 PIXEL PURITY INDEX

The Pixel Purity Index (PPI) is a means of finding the most "spectrally pure," or extreme, pixels in multispectral and hyperspectral images [12]. The PPI is a "counting system" to which the number of times each pixel within the scene result. Classified are designed as purest. Only MNF Band 1- MNF Band 4 was selected as input when running the PPI. This was because MNF Band 5- MNF Band 10 with low Eigenvalue only had little information and contained a lot of noise which could decrease the accuracy of the classification.

Figure 5. PPI Image

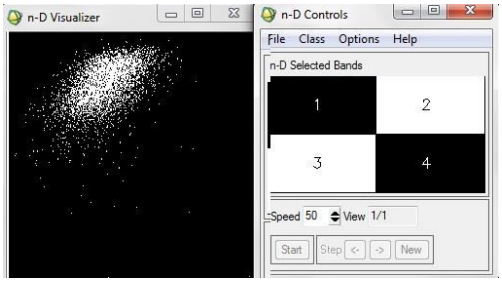

Figure. 6 Scattered plots of the purest pixels from bands 1 and 4

3.3 n-D Visualization

In this session, data (or spectral) was assumed as points in an n-dimensional scattered plot, where n referred to the number of bands. The data for a given pixel corresponding to a spectral reflectance for that given pixel. n-space was used to estimate the number of spectral end members and their pure spectral signature and to help to understand the spectral. The goal is to use principal component analysis to translate and/or rotate the original axis so that the original brightness characteristics of the materials which make up that signature. Image generated from PPI was used as the input in this stage, then different classes generated from the n-Dimensional visualizer were compared to the spectral library to identify each class, After the n-D Visualizer was identified, the spectra for each class were saved into a new spectral library file for use during SAM classification values are redistributed onto a new set of axis or dimension as shown in Figure 7, [8].

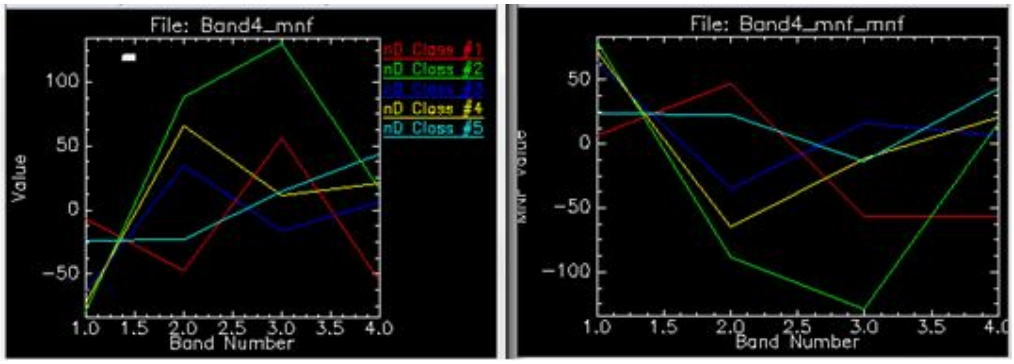

Figure 7. n-dimensional scattered plot

3.4 SPECTRAL ANGLE MAPPER (SAM)

The SAM assume that the data to be classified have been reduced to apparent reflectance. Is an automated method for comparing image spectra to individual spectra [12]. The algorithm determines the similarity between two spectra by calculating the "spectral angle" between them, the algorithm compares the angle (α) between the reference spectrum (r) and the hyperspectral images pixel measurement vector (t) in n-dimensions

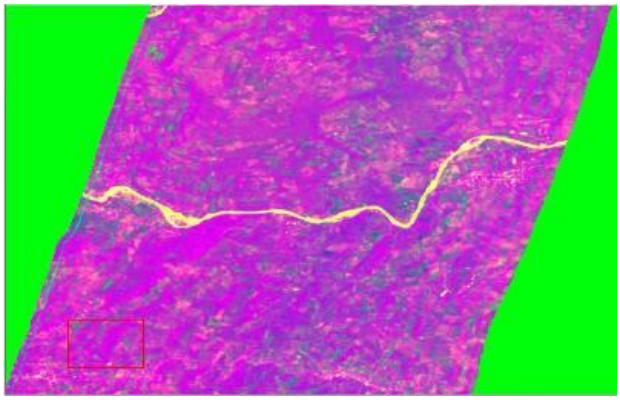

Figure 8. Spectral Angle Mapper

3.5 SPECTRAL UNMIXING ANALYSIS

To identify various pure materials and to determine their spatial proportion from remotely sensed data, the spectral mixing process has to be properly modelled. Once the spectral mixing process is modelled, the model can be inverted to derived the spatial proportions and spectral properties of pure materials It can be expressed as follows; where is a J-dimension reflectance (or digital number) vector, Fij is an L dimension fraction vector, M is a KxL end member spectral matrix, and ϵij is a K-dimension error vector presenting a residual error. The goal of spectral unmixing is to solve for with and M known.

3.1 Title and authors

The title of the paper is centered 17.8 mm (0.67") below the top of the page in 24-point font. Right below the title (separated by single line spacing) are the names of the authors. The font size for the authors is 11pt. Author affiliations shall be in 9 pt.

3.2 Body paragraphs

The main text for your paragraphs should be 10pt font. All body paragraphs (except the beginning of a section/sub-section) should have the first line indented about 3.6 mm (0.14").

3.1.1 Figures and Tables

Place illustrations (figures, tables, drawings, and photographs) throughout the paper at the places where they are first discussed in the text, rather than at the end of the paper. Number illustrations sequentially (but number tables separately). Place the illustration numbers and caption under the illustration in 10 pt font. Do not allow illustrations to extend into the margins or the gap between columns (except 2-column illustrations may cross the gap). If your figure has two parts, include the labels “(a)” and “(b)”.

3.5 SPECTRAL UNMIXING ANALYSIS

To identify various pure materials and to determine their spatial proportion from remotely sensed data, the spectral mixing process has to be properly modelled. Once the spectral mixing process is modelled, the model can be inverted to derived the spatial proportions and spectral properties of pure materials It can be expressed as follows; $R_{ij} = MF_{ij} + \epsilon_{ij}$ where R_{ij} is a J- dimension reflectance (or digital number) vector, F_{ij} is an L dimension fraction vector, M is a KxL end member spectral matrix, and ϵ_{ij} is a K-dimension error vector presenting a residual error. The goal of spectral unmixing is to solve for F_{ij} with R_{ij} and M known.

4. EXPERIMENTAL ANALYSIS OF RESULT AND DISCUSSION 4.1 ANALYSIS OF RESULT

When MNF transformation was completed, an Eigenvalue plot (Figure 2) was shown and three MNF-transformed bands (Figure 4) were displayed. From the MNF results, the first three transformed bands (MNF1-3) contained more information and the spatial coherent decreases significantly with the increase of MNF bands number. In MNF bands, the information decreased drastically less than the first three bands. (Figure 1, MNF 4-9).

- The first principal component (Eigenvalues λ_1) of the data account for 78.44% of the entire hyperspectral dataset (Table 2).
- Component 2 account for 13.63% of the remaining variance.
- Component 3 account for 2.53% of the remaining variance,
- Cumulatively, these first three principal components account for 94.60% of the variance.
- The 4th component account for another 2.00%, bring about a total of 96.60% of the variance explained by the first four components. (Table 2)
- Therefore, the ten-band hyperspectral data has been compressed into just four new principal images (or bands) that explain 96.60% of the variance.

4.2 DISCUSSION

The noise in the hyperspectral dataset is separated from the useful information. MNF output bands that contain useful image information have an eigenvalue and order of magnitude greater than those that contain mostly noise, (Table 1, column 6). In this study, the 19 MNF bands were selected for further analysis. (Figure 1) A graph of the eigenvalues by band reveals that the first four Eigen-images contain most of the valuable information.

REFERENCES

[1] AFH (1993). The Spectral Image Processing System (SIPS)–Interactive Visualization and Analysis of Imaging Spectrometer Data. Rem. Sensing Environ. 44: 145-163.
[2] Beck R (2003). EO-1 User Guide, Version 2.3., University of Cincinnati.
[3] Boardman JM (1993). Automated spectral unmixing of AVRIS data using convex geometry concept: In summaries, Fourth JPL Airborne Geoscience Workshop
[4] B. Toufik and N. Mokhtar, "The wavelet transform for image processing applications,", Laboratory of Non-Destructive Testing, Jijel University.
[5] Chen CM (2000). Comparison of principal component analysis and Minimum Noise Fraction transformation for reducing the dimensionality of hyperspectral imagery. Geo. Res., 33: 163-178.
[6] Green AA, Berman M, Switzer P, Craig MD (1988). A transformation for ordering multispectral data in terms of image quality with implications for noise removal: IEEE Trans. Geos. Remote Sensing, 26(1): 65-74.
[7] Lillesand, Thomas M.et al. (2007). Remote sensing and image interpretation
[8] Lu. G.Y. and Wong, D.W. (2008) An adaptive inverse-distance weighting spatial interpolation technique, computer and Geosciences,34,1044-1055
[9] Mustard, J.F. and sunshine, J.M. (1999). Spectral analysis for earth science.
[10] Pearlman JS, Barry PS, Segal CC, Shepanski J, Beiso D, Carman SL (2003). Hyperion, a SpaceBased Imaging Spectrometer. IEEE Trans. Geos. Remote Sensing, 41(6): 1160-1173.
[11] Pour BA, Hashim M, Marghany M (2011). The Earth Observing-1 (EO-1) satellite data for geological mapping, the southeastern segment of the central Iranian volcano Belt, Iran... J. Geralds, "Sega Ends Production of Dreamcast," vnunet.com, para. 2, Jan. 31, 2001. [Online]. Available: http://nl1.vnunet.com/news/1116995. [Accessed: Sept. 12, 2004]. (General Internet site)

[12] Kruse FA, Boardman JW, Lefkoff AB, Heidebrecht KB, Shapiro AT, Barloon PJ,
[13] Goetz Verbyla, David (1995). Satellite remote sensing of natural resource
[14] Song, C Woodcock, CE., seto, K.C et al (2001) Classification and change detection using Landsat
[15] J.R Jenson, Introductory Digital Image Processing, 3rd ed., Prentice-Hall, 1994

AUTHOR

Dahiru Mohammed Zakari received the HND and PGD in Surveying and Geoinformatics in Federal Polytechnic, Mubi and Federal University of Technology, Yola in Adamawa State, Nigeria in 1999 and 2008 and M.S. degrees in Remote Sensing from Universiti Teknologi Malaysia in 2014 respectively. During 2009 -2021, he Work with the Department of Surveying and Geoinformatics, School of Environmental Science, Jambutu Campus, Adamawa State Polytechnic, Nigeria.